

Experimental study of thermodynamic assessment of a small scale solar thermal system



H.U. Helvaci*, Z.A. Khan

Bournemouth University, Faculty of Science and Technology, Bournemouth, Nano Corr., Energy and Modelling Research Group, BH12 5BB, UK

ARTICLE INFO

Article history:

Received 7 January 2016
Received in revised form 17 March 2016
Accepted 19 March 2016
Available online 26 March 2016

Keywords:

Solar energy
ORC
HFE 7000
Flat plate collector
Exergy

ABSTRACT

In this study, a scaled solar thermal system, which utilises HFE 7000, an environmentally friendly organic fluid has been designed, commissioned and tested to investigate the system performance. The proposed system comprises a flat-plate solar energy collector, a rotary vane expander, a brazed type water-cooled condenser, a pump and a heat recovery unit. In the experimental system, the flat-plate collector is employed to convert HFE-7000 into high temperature superheated vapour, which is then used to drive the rotary vane expander, as well as to generate mechanical work.

Furthermore, a heat recovery unit is employed to utilise the condensation heat. This heat recovery unit consists of a domestic hot water tank which is connected to the condenser. Energy and exergy analysis have been conducted to assess the thermodynamic performance of the system. It has been found that the collector can transfer 3564.2 W heat to the working fluid (HFE 7000) which accounts for the 57.53% of the total energy on the collector surface. The rotary vane expander generates 146.74 W mechanical work with an isentropic efficiency of 58.66%. In the heat recovery unit, 23.2% of the total rejected heat (3406.48 W) from the condenser is recovered in the hot water tank and it is harnessed to heat the water temperature in the domestic hot water tank up to 22.41 °C which subsequently will be utilised for secondary applications. The net work output and the first law efficiency of the solar ORC is found to be 135.96 W and 3.81% respectively. Exergy analysis demonstrates that the most exergy destruction rate takes place in the flat plate collector (431 W), which is the thermal source of the system. Post collector, it is followed by the expander (95 W), the condenser (32.3 W) and the pump (3.8 W) respectively. Exergy analysis results also show that the second law efficiency of the solar ORC is 17.8% at reference temperature of 15 °C. Parametric study analysis reveals that both increase in the expander inlet pressure and the degree of superheat enhances the thermodynamic performance of the solar ORC.

© 2016 The Authors. Published by Elsevier Ltd. This is an open access article under the CC BY-NC-ND license (<http://creativecommons.org/licenses/by-nc-nd/4.0/>).

1. Introduction

Large scale energy utilisation has become a vital concern due to the increase in the demand of energy use in the last decades. At the same time, use of conventional energy sources such as fossil fuels has brought many environmental problems. Climate change and global warming, which is the main issues resulted from the release of harmful substances into the atmosphere have been forcing us to explore alternative energy sources [1,2].

Solar energy is a free, clean and abundant alternative energy source and it can be utilised by means of solar photovoltaic (PV) and solar thermal systems [3]. Although solar PVs have become one of the most representative ways of electricity generation in

rural areas, high costs of PV panels, limited efficiency and requirement of expensive batteries are the main disadvantages of such systems [4].

Medium and high temperature solar thermal systems where concentrated solar collectors such as parabolic through [5,6], linear Fresnel [7] and parabolic dish [8] are used have been suggested and developed over the last decades. However, these systems need high initial cost and complex tracking devices [9].

An organic Rankine cycle, which has the same system configuration as conventional Rankine cycle uses organic substances (refrigerants or hydrocarbons) instead of water as a working fluid [10]. Using organic fluids with a lower boiling temperature than water allows these systems to utilise low temperature heat from various renewable energy sources [11]. As a result, non-concentrated low temperature flat plate collectors can be employed in organic Rankine cycles to generate power and heat simultaneously [12].

* Corresponding author at: Faculty of Science and Technology, Fern Barrow, Talbot Campus, Bournemouth University, Poole, Dorset BH12 5BB, UK.

E-mail address: hhelvaci@bournemouth.ac.uk (H.U. Helvaci).

Nomenclature

A	area (m^2)	col	collector
CFCs	chlorofluorocarbons	$cond$	condenser
e	specific exergy (J/kg)	$dest$	destruction
\dot{E}_x	exergy rate (W)	exp	expander
h	enthalpy (J/kg)	fin	final
HCFCs	hydrochlorofluorocarbons	in	inlet
HFCs	hydrofluorocarbons	int	initial
HFEs	hydrofluoroethers	out	outlet
L	litre	p	plate
m	mass (kg)	rec	recovery
\dot{m}	mass flow rate (kg/s)	s	isentropic
I	solar radiation (W/m^2)	sat	saturation
ORC	organic Rankine cycle	sol	solar
\dot{Q}	heat transfer rate (W)	st	storage
\dot{Q}_u	useful heat gain (W)	u	useful
PFCs	perfluorocarbons	w	water
PV	photovoltaic	wf	working fluid
RO	reverse osmosis	0	reference (dead) state
s	entropy (J/kg K)		
t	time (s)		
T	temperature ($^\circ\text{C}$)		
V	volume (m^3)		
\dot{W}	work rate (W)		

Subscripts

amb ambient

Greek symbols

ρ	density (kg/m^3)
η	first law efficiency
ε	second law efficiency

Various refrigerants have been used and analysed in solar organic Rankine cycles for both mechanical work and heat generation. Manolakas et al. [13–15] suggested a low-temperature solar thermal power system utilising HFC-134a for reverse osmosis (RO) desalination. The mechanical work generated in the expander of the cycle is used for the pumping purpose of the RO desalination. An experimental study of solar organic Rankine cycle using HFC-245fa was conducted by [9]. In this study, two stationary collectors which are flat-plate and evacuated tube were employed in the experiments. Collector efficiencies of evacuated tube and flat-plate were found 71.6% and 55.2% respectively. The solar thermal power system, including heat regeneration was also analysed in [16]. In this study R-245fa was used as a working fluid of the cycle and maximum thermal efficiency of 9% was obtained with heat regeneration [16]. In another study, recuperative solar thermal cycle with HFC-245fa was designed and constructed by Wang et al. [17]. It was found that the recuperator did not have any effect on the improvement of the system thermal efficiency, which was about 3.67% [17]. Not only pure refrigerants but also zeotropic mixtures were studied in solar thermal systems. Wang et al. [18] carried out an experimental study of low-temperature solar thermal system considering pure HFC-245fa, a zeotropic mixture of (HFC-245fa/HFC-152a, 0.9/0.1) and another mixture of (HFC-245fa/HFC-152a, 0.7/0.3). Since the efficiency of the collector and the system found higher in zeotropic mixtures it is concluded that zeotropic mixtures have a potential to improve the overall efficiency of such systems [18].

In addition to refrigerants, CO_2 which is a natural fluid was also examined in many solar powered supercritical cycle studies. Zhang et al. [19] carried out an experimental study to examine a solar thermal power cycle performance where supercritical CO_2 was utilised as a working fluid. They concluded that the heat collection efficiency of the collector reached 70% and the system achieved 8.78–9.45% power generation efficiency [19]. Another solar thermal power system using CO_2 was proposed and built in Yamaguchi

et al. [20]. A throttling valve was used in order to simulate pressure drop in turbine and to study the system performance. They concluded that solar collector can be used for heating of CO_2 in the cycle up to 165 $^\circ\text{C}$. The power generation efficiency of the cycle is estimated for 25% and the heat recovery efficiency for 65% [20].

Thermodynamic analysis considering energy and exergy methods is an essential tool to investigate not only the quantity, but also the quality of energy used in a system [21] and it is also important for designing and analysing thermal systems [22].

Many studies, including energy and exergy analysis of solar thermal power systems have been conducted by various researchers. Singh et al. [23] conducted the first and second laws analysis of a solar thermal power system integrated with parabolic through collector. It is reported that the highest energy loss occurred in the condenser whereas parabolic through collector/receiver component was found to be the source of main exergy losses in the system [23]. Exergy analysis of parabolic through collector combined with steam and organic Rankine cycle has been examined by [24]. Among the considered various refrigerants R-134a gives the best exergetic performance with an efficiency of 26% [24]. Combined exergetic and exergoeconomic analysis of an integrated solar cycle system was carried out by [25]. In this study, genetic algorithm was utilised for the optimisation procedure to minimise the investment cost of equipment and the cost of exergy destruction. Results showed that for optimum operation, total cost rate decreased by 11% [25]. Elsafi [26] applied exergy and exergoeconomic analysis methods to a commercial-size solar power plant using parabolic through collectors. Exergy and exergy costing balance equations are formulated for each component. It is reported that the highest exergy destruction was calculated for the solar field (63,319 kW) and it was followed by the condenser (4187.5 kW) [26].

Although numerous experimental and simulation studies have been reported on the thermal performance evaluation of small scale solar organic Rankine cycles, detailed thermodynamic analysis of such systems considering energy and exergy methods has

been of interest to a limited number of papers. Previously, a flat plate solar collector was numerically modelled and simulated to investigate the collector performance for two working fluids (HFC-134a and HFE-7000) under various operating conditions [27]. In this study, a scaled solar thermal cycle where the flat plate solar collector is utilised as a direct vapour generator of the system was designed and commissioned. An experimental study using working thermo-fluid (HFE-7000) was performed. To understand the performance characteristics of the solar ORC, the first and second law analyses of each component, as well as the whole system, is evaluated by using experimental data. To utilise the rejected heat from the system, the solar ORC is integrated with a heat recovery unit and the findings is represented in the energy analysis of the system.

In the exergy analysis of the solar organic Rankine cycle, exergy destruction rate and the second law efficiency of each component is investigated. Furthermore, a parametric analysis is carried out in order to evaluate the effects of expander inlet pressure and the degree of superheat on the system performance.

2. Working fluids for solar ORC

Working fluid selection is an important task in ORCs since it affects the performance of a system, as well as it is essential for environmental concerns [28]. Chlorofluorocarbons (CFCs) and hydrochlorofluorocarbons (HCFCs) are conventional refrigerants and they have high potential to deplete the ozone layer [29]. Therefore, perfluorocarbons (PFCs) and hydrofluorocarbons (HFCs) have been used as a promising alternative since they have near-zero ozone depletion potential (ODP). However, PFCs and some HFCs have a relatively high global warming potential [30]. Alternatively, hydrofluoroethers (HFEs) which have zero ozone depletion factor and low global warming potential can be used as candidates for CFCs, HCFCs and PFCs [31] and HFEs can be utilised as a working fluid in ORCs [32,33]. Table 1 shows the properties of conventional and novel organic fluids that have been used in ORCs and refrigeration cycles.

In this study, HFE-7000 is utilised as a working fluid of the solar thermal cycle as it has zero ODP, relatively low value of GWP and reasonable boiling temperature.

3. Experimental bench testing

Experimental system evaluates the performance of a small scale solar thermal technology which employs HFE 7000 as a working fluid.

3.1. Description of the system

The proposed experimental solar thermal system consists of two units: (i) Solar organic Rankine cycle unit which has main components of a flat-plate solar collector, an air motor, a plate-type heat exchanger, a liquid reservoir and a positive displacement pump. (ii) Heat recovery unit with a domestic hot water tank, as

shown in Fig. 1. The test rig operates on an ORC principle where the working fluid (HFE-7000) is compressed by the pump and is sent to the flat-plate collector (Fig. 1, state 2). The solar radiation is converted to heat in the collector and it is transferred to the high pressure fluid in the collector tubes where the phase change occurs. Therefore, the collector acts as an evaporator, in other words pressurised vapour generator of the cycle. The fluid might leave the collector as liquid–vapour mixture, saturated vapour or superheated vapour depending on the operating conditions of the system (Fig. 1, state 3).

Pressurised vapour is directed to the turbine where the fluid expands and generates mechanical work. Then, the lower pressure exhaust vapour at the end of the expander goes to the condenser to reject some of its heat from the system (Fig. 1, state 4). The mains water (with an average temperature of 10–13 °C) is used to cool the working fluid and turn it into the liquid state in the condenser (Fig. 1, state 1). Then, liquefied working fluid is pumped again into high pressure to complete the cycle. As shown in Fig. 1 the condenser outlet is connected to the heat recovery unit where the domestic hot water tank is utilised to recover the energy content of rejected heat from the solar ORC.

Flat-plate collector which is formed of a glass cover, a stainless steel absorber plate and a 56 m copper tube in length is used in the experiments. A diaphragm pump which is employed in the experiments to compress the working fluid and it can provide a maximum flow rate of 3 L/min. To adjust the flow rate of the fluid by throttling on the discharge side of the pump a valve is mounted in the system. The condenser utilised in the experiments is a brazed plate heat exchanger and it is fed by mains water to cool the working fluid as mentioned previously. Twelve litre vertical liquid reservoir which provides a steady supply of the fluid was placed after the condenser. A rotary vane air motor is modified and used as an expander of the cycle. Rotary vane expanders can be utilised in ORC applications [37] since they have simpler structure, easy manufacturing and low cost [28]. The air motor used in the experiments can supply a maximum power output of 0.8 kW and maximum rotational speed of 4000 rpm. A 118 L copper-coiled hot water tank is selected to deliver the energy of the pre-heated water coming out of the condenser to the stagnant, stored water in the storage tank (Fig. 1, heat recovery unit).

3.2. Experimental method

Leak test of the system is one of the most important tasks as it affects the overall efficiency and the safety of the system. The system leak test was conducted to examine if there was any leakage somewhere in the cycle. Special attention was given to couplings, joints and the components of the cycle. Initially, a vacuum pump was connected to the system via a vacuum line to pull a vacuum in the cycle. Vacuum gauge was mounted to the system to record the pressure. The system was evacuated and left for 24 h to observe for any leakage through changes in the system pressure. As no change observed in the pressure of the system the line was shut off and the vacuum pump was disconnected. Then, the same line was connected to the working fluid cylinder and the valve was turned on for the subsequent flow of the working fluid into the cycle due to the pressure difference between the system and the working fluid cylinder. 8 kg (5.7 L) of HFE-7000 was introduced to the system. Evaluation of the amount of working fluid to be charged relies on the calculation of the volume of each component and the tube of the cycle. Since the vapour density of the fluid is relatively smaller than the liquid density, the regions in the components and the pipe where the fluid turns into vapour is neglected in the calculation. After the calculation of the volume of each component and the tube, the total volume of the system is multiplied by the fluid density to evaluate the total mass of the working fluid

Table 1
Properties of conventional and novel organic fluids.

Working fluid		$T_{boiling}^a$ (°C)	ODP	GWP	Reference
CFC	R-11	23.37	1	5800	[34]
HCFC	R-141b	31.67	0.12	725	[35]
HFC	R-245fa	14.81	0	950	[35]
HFE-7000	RE347mcc	34	0	450	[30]

^a Fluids boiling temperature data was taken from REFPROP 9.1 programme [36] at 1 bar.

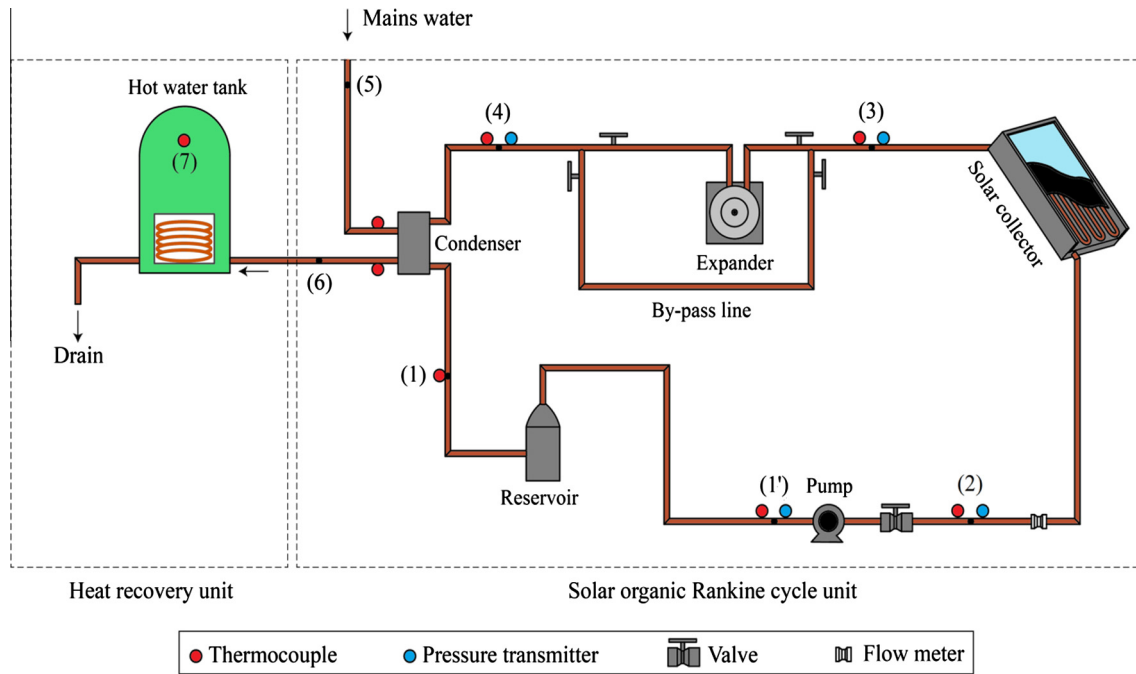


Fig. 1. Schematic layout of the solar thermal system.

[38]. Then, the condenser and the pump were turned on to circulate the water and the fluid through the system without supplying any heat input to check the system consistency and safety. The data acquisition unit was turned on to monitor and record the temperature, pressure and flow rate data. In order to supply steady radiant energy to the collector a solar simulator was utilised in the experiment. Initially, the solar simulator was switched on and the expander by-pass line was opened so the fluid reaches the condenser directly after the solar collector. Once the fluid reaches the vapour conditions the by-pass line was closed and let the fluid pass through the expander. The fluid expands in the rotary vane air motor and produces mechanical work by rotating the motor shaft. Then it is condensed by the help of cooling water in the condenser and is sent back to the solar collector.

In the data measurement system, K-type thermocouples and pressure transmitters are mounted in the experimental prototype to measure temperature and pressure values of HFE-7000 and temperature values of water at specified points as represented in Fig. 1. Thermocouples and pressure transmitters have an accuracy of ± 0.18 and $\pm 0.5\%$ respectively. A turbine flow meter with an accuracy of 2% was used to measure the volumetric flow rate of the fluid and the measured flow rate was multiplied by the fluid density (ρ_{wf}) to calculate the mass flow rate of the working fluid. All the data is taken and recorded in a time step of 10 s and transmitted to the computer by an Agilent 34972A data acquisition unit. Although it was not shown in Fig. 1, a pyranometer is mounted in the collector to measure the average irradiance on the collector surface. The collector was marked at every 48 cm in height and at every 58 cm in width. 10 kW heat was supplied from the solar simulator and the radiation data was measured at the specified points via the pyranometer on the collector surface. Detailed representation of the measured points on the collector surface can be found in [27]. During the measurements the solar simulator was located 2 m away from the collector surface and the measured radiation was assumed to be constant at each point. According to the measurement results the calculated average radiation on the collector surface was found to be 890 W/m^2 . This value of average radiation on the collector surface is in the range of solar radiation intensity

which is used both in experimental and theoretical studies reported previously [9,17,20,24,39].

4. Thermodynamic analysis

Based on the measured temperature, pressure and flow rate values of the working fluid at the defined locations (Fig. 1) it is possible to gain an understanding of performance of the proposed solar thermal cycle by applying the first and second law analysis of thermodynamics. Since the proposed solar thermal system is a closed loop cycle the calculations rely on the application of mass, energy and exergy balance equations at steady state on the each component.

The balance equations in the rate form for any open system at steady state, steady-flow condition with negligible kinetic and potential energy changes are expressed in Eqs. (1)–(3) [40,41].

$$\sum \dot{m}_{\text{in}} = \sum \dot{m}_{\text{out}} \quad (1)$$

where \dot{m} is the mass flow rate and the subscripts “in” and “out” represent inlet and outlet respectively.

The energy balance equation can be defined as:

$$\dot{Q} - \dot{W} = \sum \dot{m}_{\text{out}} h_{\text{out}} - \sum \dot{m}_{\text{in}} h_{\text{in}} \quad (2)$$

In Eq. (2), h is the enthalpy, \dot{Q} and \dot{W} are the heat and work transfer rates of the system.

The exergy balance equation is expressed as:

$$\dot{E}x_{\text{heat}} - \dot{W} + \sum \dot{E}x_{\text{in}} - \sum \dot{E}x_{\text{out}} = \sum \dot{E}x_{\text{dest}} \quad (3)$$

where $\dot{E}x$ indicates the exergy rate and the subscript “dest” represents the exergy destruction rate of the system.

In Eq. (3), $\dot{E}x_{\text{heat}}$ represents the exergy transfer rate by heat and it can be calculated as:

$$\dot{E}x_{\text{heat}} = \sum 1 - \left(\frac{T_0}{T} \right) \dot{Q}_j \quad (4)$$

and the specific exergy (kJ/kg) is given by:

Table 2

Balance equations for each component [21,41,42].

Component	Mass balance equations	Energy balance equations	Exergy balance equations
Collector	$\dot{m}_2 = \dot{m}_3 = \dot{m}_{wf}$	$\dot{Q}_u = \dot{m}_{wf} \times (h_3 - h_2)$	$\dot{E}x_{dest,col} = (\dot{E}x_2 - \dot{E}x_3) + IA_{col} \left[1 - \frac{T_0}{T_p} \right]$
Expander	$\dot{m}_3 = \dot{m}_4 = \dot{m}_{wf}$	$\dot{W}_{exp} = \dot{m}_{wf} \times (h_3 - h_4)$	$\dot{E}x_{dest,exp} = (\dot{E}x_3 - \dot{E}x_4) - \dot{W}_{exp}$
Condenser	$\dot{m}_4 = \dot{m}_1 = \dot{m}_{wf}$ $\dot{m}_5 = \dot{m}_6 = \dot{m}_w$	$\dot{Q}_{cond} = \dot{m}_{wf} \times (h_4 - h_1)$ $\dot{Q}_{cond} = \dot{m}_w \times (h_{w,out} - h_{w,in})$	$\dot{E}x_{dest,cond} = (\dot{E}x_4 - \dot{E}x_1) + (\dot{E}x_5 - \dot{E}x_6)$
Pump	$\dot{m}_{1'} = \dot{m}_2 = \dot{m}_{wf}$	$\dot{W}_{pump} = \dot{m}_{wf} \times (h_2 - h_{1'})$	$\dot{E}x_{dest,pump} = (\dot{E}x_{1'} - \dot{E}x_2) + \dot{W}_{pump}$

$$e = (h - h_0) - T_0(s - s_0) \quad (5)$$

Therefore, the total exergy rate (W) can be calculated by using the following equation:

$$\dot{E}x = \dot{m} \times e \quad (6)$$

The balance equations (mass, energy and exergy) for each component are derived with the following assumptions by using Eqs. (1)–(6) and given in Table 2.

- All the components in the system are at steady state.
- Changes in kinetic and potential energy are neglected.
- The reference-dead state has a pressure of $P_0 = 1$ bar = 101.325 kPa and temperature of 15 °C.

In the exergy destruction equation of the collector, the term $(IA_{col} [1 - \frac{T_0}{T_p}])$ represents the exergy rate of the solar radiation absorbed on the collector surface where I is the incoming solar radiation, A_{col} is the collector area, T_0 and T_p are the dead state temperature and the collector plate temperature respectively [42].

Furthermore, water flow rate through the condenser is evaluated via the energy balance in the condenser. Considering the steady state conditions:

$$\dot{Q}_{cond} = \dot{m}_{wf} \times (h_4 - h_1) = \dot{m}_w \times (h_{w,out} - h_{w,in}) \quad (7)$$

and water mass flow rate can be evaluated as:

$$\dot{m}_w = \frac{\dot{Q}_{cond}}{(h_{w,out} - h_{w,in})} \quad (8)$$

where \dot{Q}_{cond} represents the amount of heat rate rejected in the condenser and $h_{w,out}$ and $h_{w,in}$ represents the outlet and inlet enthalpy of the water respectively.

4.1. Energy efficiencies

First law efficiency, in other words energy efficiency of a system or system component represents the ratio of energy output to the energy input and it can be calculated as [43];

$$\eta = \frac{\text{Desired output energy}}{\text{Supplied energy input}} \quad (9)$$

Flat-plate collector

Collector efficiency can be defined as the ratio of useful collected heat rate of the working fluid (\dot{Q}_u) to the solar radiation absorbed on the collector surface (Q_{sol}).

$$\eta_{col} = \frac{\dot{Q}_u}{Q_{sol}} \quad (10)$$

where

$$Q_{sol} = I \times A_{col} \quad (11)$$

Expander

$$\eta_{exp} = \frac{h_3 - h_4}{h_3 - h_{4,s}} \quad (12)$$

Solar ORC

The thermal (first law) efficiency of the proposed solar organic Rankine cycle can be expressed as the ratio of the net work output to the useful heat gain of the working fluid and it is calculated as below:

$$\eta_{sorc} = \frac{\dot{W}_{net}}{\dot{Q}_u} = \frac{\dot{W}_{exp} - \dot{W}_{pump}}{\dot{Q}_u} \quad (13)$$

Heat recovery

Heat recovery efficiency can be expressed as the ratio of the amount of heat which is gained by the water in the hot water tank to the maximum amount of heat that can be utilised from the condenser.

$$\eta_{rec} = \frac{\dot{Q}_{st}}{\dot{Q}_{cond}} \quad (14)$$

where

$$\dot{Q}_{st} = \frac{m_{w,st} \times C_{p,w} \times (T_{w,st,final} - T_{w,st,initial})}{t_{exp}} \quad (15)$$

$$m_{w,st} = V_{st} \times \rho_w \quad (16)$$

4.2. Exergy efficiencies

Second law efficiency is defined as the ratio of the output exergy to the exergy input and it is given as:

$$\varepsilon = \frac{\text{Exergy output}}{\text{Exergy input}} \quad (17)$$

Flat-plate collector

Exergy efficiency of the collector is the ratio between the exergy gain of the fluid and exergy content of the incoming solar radiation and it is calculated as:

$$\varepsilon_{col} = \frac{\dot{E}x_3 - \dot{E}x_2}{IA_{col} \left(1 - \frac{T_0}{T_p} \right)} \quad (18)$$

Expander

$$\varepsilon_{exp} = \frac{\dot{W}_{exp}}{(\dot{E}x_3 - \dot{E}x_4)} \quad (19)$$

Pump

$$\varepsilon_{pump} = \frac{\dot{E}x_2 - \dot{E}x_{1'}}{\dot{W}_{pump}} \quad (20)$$

Condenser

$$\varepsilon_{cond} = \frac{\dot{E}x_6 - \dot{E}x_5}{(\dot{E}x_4 - \dot{E}x_1)} \quad (21)$$

Solar ORC

The exergy efficiency of the system is written as;

$$\varepsilon_{sorc} = \frac{\dot{W}_{net}}{\dot{E}x_{in}} \quad (22)$$

Taking the exergy of the solar radiation as an exergy input to the solar organic Rankine cycle Eq. (22) becomes;

$$\varepsilon_{\text{sorc}} = \frac{\dot{W}_{\text{net}}}{IA_{\text{col}} \left(1 - \frac{T_0}{T_p}\right)} \quad (23)$$

Furthermore, in order to calculate the relative ratio of the exergy destruction of j_{th} component to the total exergy destruction, the following expression is used:

$$RI_j = \frac{\dot{E}x_{\text{dest},j}}{\dot{E}x_{\text{dest,tot}}} \quad (24)$$

5. Results and discussion

In performing the first and second law analysis of the small scale solar thermal system, the experimental values of temperature (°C), pressure (bar) and flow rate (kg/s) were collected in order to determine fluid state where gas refers to superheated vapour, specific enthalpy (kJ/kg), specific exergy and exergy rate associated with each of the state of the proposed cycle (Table 3). T–s diagram of the working fluid at each state is also shown in Fig. 2.

During the experiments the average value of $I = 890 \text{ W/m}^2$ of solar radiation was supplied to the collector and the flow rate of the working fluid was held constant with an average value of 0.022 kg/s . In the analysis, the reference dead state conditions for temperature and pressure are taken to be 288 K and 1 bar respectively. All the data monitored and analysed in this study when the expansion takes place in the expander and thermodynamic state properties of HFE 7000 were extracted from Ref. [36].

5.1. Energy analysis results

In this section the performance of the proposed solar thermal cycle through the collector efficiency, expander efficiency, heat recovery efficiency, net work output and the system thermal efficiency are examined by the measured temperature, pressure and flow rate values.

Energy rate analysis of the solar collector is shown in Table 4.

The energy received on the collector surface is calculated as 6194.4 W with the help of Eq. (11). In the collector, 57.53% of this energy is utilised to heat the working fluid from 19.1°C at the collector inlet to 45.41°C at the collector outlet. The working fluid temperature at the outlet of the collector is almost 4°C higher than the corresponding saturation temperature ($T_{\text{sat}} = 41^\circ\text{C}$) of the fluid. This shows that with the constant flow rate of 0.022 kg/s , HFE-7000 was able to finish its phase change and leave the collector as a superheated vapour state (Fig. 2). Since HFE 7000 is a dry fluid according to its saturation vapour line, a small degree of superheating would not cause any risk of encountering some portion of liquid in the expander. Furthermore, higher degree of superheating at the collector outlet might lead to an excessive increase in the

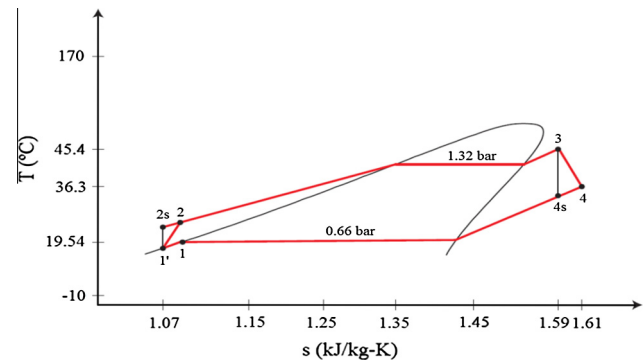


Fig. 2. T–s diagram of the experimental results.

Table 4
Energy rate analysis of the solar collector.

Parameters	Value	Unit
Energy received by the collector (Q_{sol})	6194.4	W
Useful heat gain of the fluid (Q_u)	3564.2	W
Collector energy loss ^a	2907.8	W
Collector efficiency (η_{exp})	57.53	%

^a $Q_{\text{sol}} - Q_u$.

Table 5
Energy rate analysis of the expander.

Parameters	Value	Unit
Work output of the expander (\dot{W}_{exp})	146.74	W
Isentropic efficiency of the expander (η_{exp})	58.66	%

fluid temperature as well as the heat loss from the system to the atmosphere. Energy rate analysis of the expander can be found in Table 5. Assuming that the expander is adiabatic, according to Eq. (12) the isentropic efficiency of the expander and the work output are found to be 58.66% and 146.74 W respectively. This isentropic efficiency value is similar to the reported efficiency of rotary vane expander using HFE 7000 in [32].

As it can also be seen from Fig. 1, pressure loss through the condenser is neglected. Therefore, the outlet pressure of the expander also represents the condensing pressure of the cycle ($P_{\text{sat}} = 0.66 \text{ bar}$). The working fluid leaves the expander at 36.36°C and it transfers its heat to the cooling water and leaves the condenser at 19.54°C . According to the corresponding saturation temperature at 0.66 bar ($T_{\text{sat}} = 22.93^\circ\text{C}$), the fluid is below the saturation temperature, in other words it is sub-cooled at the outlet of the condenser. Then its temperature decreases to 18.73°C after the liquid reservoir. Although there is a slight decrease in pressure after the liquid reservoir, it can be seen that with the temperature of 18.73°C and a pressure of 0.57 bar , the fluid is sub-cooled at the

Table 3
Thermodynamic state properties of HFE-7000 at various points.

State (No)	Fluid type	Phase	T (°C)	P (bar)	\dot{m} (kg/s)	h (kJ/kg)	e (kJ/kg)	$\dot{E}x$ (W)
0	HFE-7000	Dead state	15	1	–	218.05	–	–
0	Water	Dead state	15	1	–	63.076	–	–
1	HFE-7000	Liquid	19.54	0.66	0.022	223.56	0.038	0.83
1'	HFE-7000	Liquid	18.73	0.57	0.022	222.57	0.084	1.86
2	HFE-7000	Liquid	19.1	1.86	0.022	223.06	0.402	8.84
3	HFE-7000	Gas	45.41	1.32	0.022	385.07	15.532	341.7
4	HFE-7000	Gas	36.36	0.66	0.022	378.4	4.542	99.98
5	Water	Liquid	13.47	0.66	0.06	56.63	–0.11	–6.6
6	Water	Liquid	26.88	0.66	0.06	112.75	1.002	60.12

outlet of the reservoir. This shows that there is no vapour flowing through the pump which might cause a cavitation problem otherwise. Since water-cooling system is used to reject some portion of heat from the solar ORC unit, it is found that in the condenser an average amount of 3406.48 W heat is transferred to the cooling water and increased its temperature from 13.47 °C to 26.88 °C. As mentioned above, in order to recover the dissipated heat the condenser outlet (Fig. 1, state 6) is connected to the hot water storage tank. This pre-heated water circulates within the coil of the water tank and delivers its heat energy to the stored cold water (Fig. 1, state 7) in the tank. Fig. 3 shows the cooling water inlet and outlet temperature and the temperature change of the stored water in the tank during the experiment. It is seen from Fig. 3 that at the beginning of the experiment stored water temperature was 16.65 °C and its final temperature reached 22.41 °C by the end of the experiment. This utilised heat in the hot water tank is supplied by the waste cooling water coming out of the condenser with an average temperature of 26.88 °C.

By using Eqs (14)–(16) heat gain rate of the hot water tank and the heat recovery efficiency of the system are calculated and the analysis results are given in Table 6. It is shown that 23.2% of the total rejected heat ($\dot{Q}_{cond} = 3.406$ kW) is recovered and is used to pre-heat the stored water in the hot water storage tank.

Consequently, the proposed solar ORC extracts 3564.2 W heat from the solar source and it converts 146.74 W of this heat to the mechanical work. Considering the average pump consumption rate in the analysis ($\dot{W}_{pump} = 10.78$ W), the net work output of the proposed solar ORC is found to be 135.96 W. Therefore, by using Eq. (13), the first law efficiency of the cycle is calculated as 3.81%. In the condenser, 3406.48 W of heat, which represent 95.5% of the total heat input of the cycle is rejected from the system. Then, 23.2% of this rejected heat is recovered in the domestic hot water tank for secondary uses.

5.2. Exergy analysis results

The exergy destruction rate and the exergetic efficiency values are represented in Table 7 and relative irreversibility of each component is represented in Fig. 4. It should be noted that heat recovery unit is neglected in the calculation of exergy analysis. Therefore, the causes of the exergy destruction in the solar ORC include flat-plate solar collector, expander, pump and condenser.

As it can be seen from Table 7 the highest exergy loss occurs in the collector (431 W) and this represents 76.68% of the total exergy

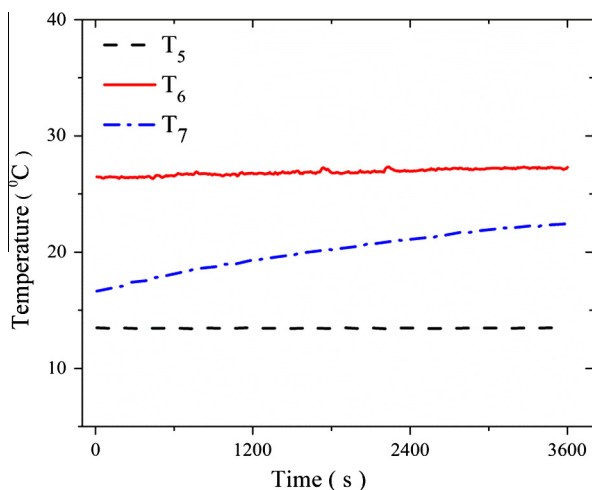


Fig. 3. Water temperature at condenser inlet, outlet and hot water tank.

Table 6

Analysis results of the heat recovery unit.

Parameters	Value	Unit
Testing time	3600	s
Initial water temperature ($T_{7,init}$)	16.65	°C
Final water temperature ($T_{7,fin}$)	22.41	°C
Total mass of water in the tank ($m_{w,st}$)	118	kg
Water specific heat capacity ($C_{p,w}$)	4.187	kJ/kg K
Total energy gain rate in the tank	2845.82	kJ
Average energy gain rate throughout the test (\dot{Q}_{st})	0.79	kW
Average rejected heat rate in the condenser (\dot{Q}_{cond})	3.406	kW
Heat recovery efficiency in the hot water tank (η_{rec})	23.2	%

Table 7

Exergy performance data for the cycle.

Component	$\dot{E}x_{dest}$ (W)	ε (%)
Solar collector	431	43.57
Expander	95	60.7
Condenser	32.3	67.3
Pump	3.8	64.73

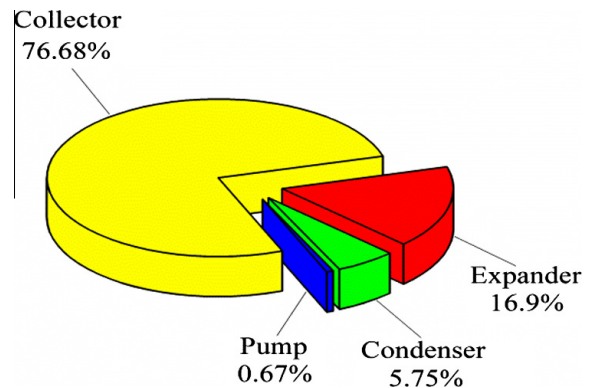


Fig. 4. Relative irreversibilities of each component.

destruction rate in the system (Fig. 4). This large amount of exergy destruction rate in the solar collector could be explained by the high difference in quality between solar radiation and the working fluid at collector operating temperature. The same trend can be found in Ref. [24,26,44] where the solar collector that represents the thermal source of the cycle is the main source of exergy destruction. The next largest exergy destruction rate appeared to be in the expander (95 W), representing 16.9% of total exergy destruction rate (Fig. 4). Then the expander is followed by condenser and pump, accounting for 32.36 W and 3.8 W respectively. The second law efficiencies of each component and the system are calculated by using Eqs. (17)–(23) and are represented in Table 7. As it can be seen from Table 7 that solar collector has the lowest second law efficiency (43.57%) due to its large exergy destruction. Another exergy efficiency value at the expander was calculated as 60.69%. This low exergetic efficiency value could be explained by the irreversibilities in the expander such as internal leakage and thermal loss [45]. This also leads a low expander isentropic efficiency which is found to be 58.66% for the present expander. Finally, according to Eq. (23) the exergy efficiency of the whole system is calculated as 17.8%. The overall exergy efficiency of the system can be improved by reducing the exergy destruction rate of the flat-plate collector and the expander as these components are the main source of the irreversibilities of the system. This will also diminish the overall exergy destruction rate of the system and will lead to an increase in the exergy efficiency of these components, as well as the whole system.

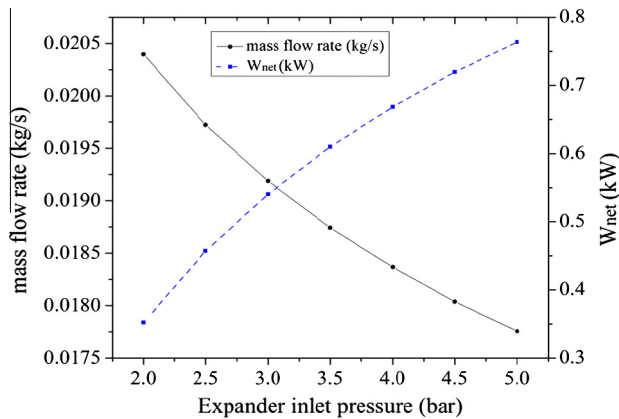


Fig. 5. Mass flow rate and net work output of the cycle versus expander inlet pressure.

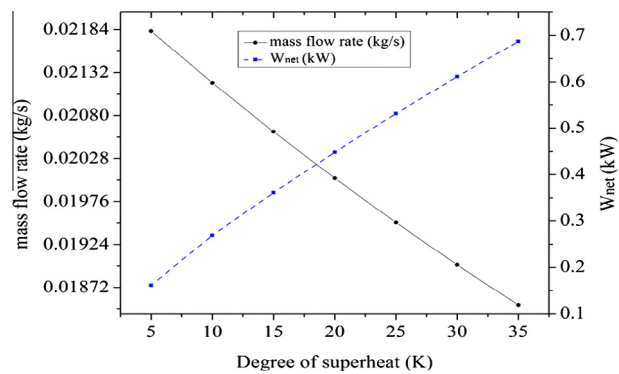


Fig. 6. Mass flow rate and net work output of the cycle versus degree of superheat.

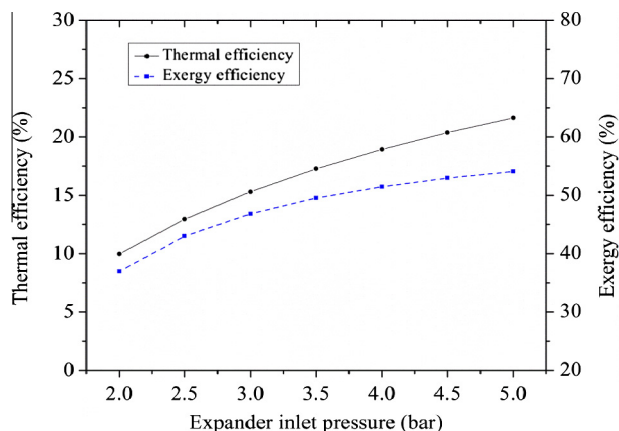


Fig. 7. Variation of the energy and exergy efficiencies of the solar ORC for various expander inlet pressure.

5.3. Parametric analysis

As a part of the analysis the effects of expander inlet pressure and the degree of superheat on the first and second law efficiency of the solar ORC are investigated. Figs. 5 and 6 demonstrate the effect of expander inlet pressure and superheat at the expander inlet on working fluid mass flow rate and the net work output of the solar ORC respectively.

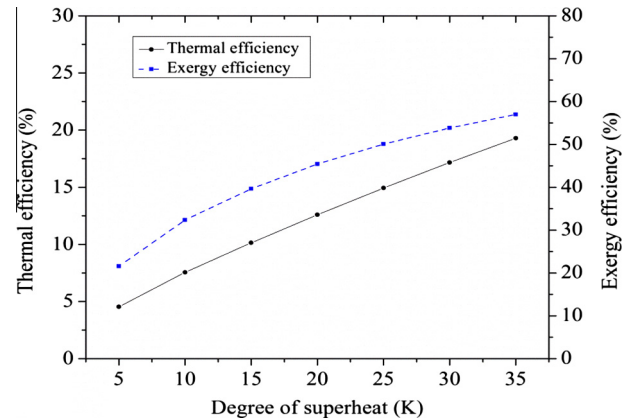


Fig. 8. Variation of the energy and exergy efficiencies of the solar ORC for various degree of superheat.

Since the incoming solar radiation and the collector efficiency were kept constant, increase in expander inlet pressure and degree of superheat reduce the working fluid mass flow rate. At the same time, increase in the both pressure and temperature leads an improvement in the enthalpy gradient at the expander which results in higher amount of net work output of the system. Fig. 7 shows the variation of the first and second law efficiency of the solar ORC with increasing expander inlet pressure.

As it can be seen from Fig. 7 that for the constant condenser pressure of 0.66 bar, when the expander inlet pressure increases from 2 bar to 5 bar, the first and second law efficiency of the system increase from 9.96% to 21.63% and from 36.95% to 54.07% respectively. As expected this trend shows that higher pressure ratio of the cycle leads to an increase in the efficiency of the system [34].

Similar trend is observed with the increasing expander inlet temperature. At the constant expander inlet pressure (1.32 bar) when the degree of superheating is increased to 35 K the thermal efficiency of the system rises and finally reaches 19.29% while the exergy efficiency reaches 56.9% (Fig. 8).

Improvements in the first and second law efficiency of the system with increasing both expander pressure and the degree of superheat could be explained by the improvement in the amount of net work output which is superior to the decrease in the flow rate of the system. However, during the parametric analysis some limitations of the cycle such as the pressure ratio of the cycle and heat losses from the collector to the ambient were neglected. For instance, in real conditions due to leakage and structural problems there should be a reasonable pressure ratio value which was stated as about 3.5 by Tchanche et al. [46]. Furthermore, it is expected that as the degree of superheating and pressure at the expander inlet increases, in other words the collector temperature increases, the higher amount of thermal losses takes place from the collector to the ambient and this would cause a decrease in the collector efficiency [27]. Therefore, it is important to conduct an optimisation study considering all the limitations mentioned above in order to define optimum operating conditions of the cycle.

6. Conclusions

In this study, a small scale solar thermal cycle which employs HFE 7000 as a working fluid is designed, commissioned and tested experimentally. The proposed cycle is comprised of solar ORC and heat recovery units. The solar ORC uses a solar flat-plate collector as an evaporator in order to supply sufficient heat to the fluid

and it acts as a direct vapour generator in the cycle. This high pressure vapour in the collector expands and generates mechanical work through the rotary vane expander. Some portion of the heat is rejected from the solar ORC in the condenser. In order to utilise this waste heat, the condenser is connected to the heat recovery unit where the domestic hot water tank is placed.

Experimental results have been discussed through the first and second law analysis of thermodynamics using mass, energy and exergy balance equations in this paper. The results reveal that the flat plate collector can provide sufficient heat to increase the working fluid temperature up to 45.41 °C and turn it into superheated vapour at the expander inlet with an average solar radiation of 890 W/m². In the energy analysis, average heat collection efficiency of the collector is estimated as 57.53%. The rotary vane expander which is used in the experiments generates average mechanical work of 146.74 W, with an isentropic efficiency of 58.66%. In the condenser 3.406 kW heat is rejected from the system and 23.2% of this condensation heat is re-used in the heat recovery unit. It is recovered to increase the temperature of 118 L water in the tank from 16.65 °C to 22.41 °C in 60 min. Exergy analysis results show that the maximum exergy destruction rate occurs in the flat plate collector with 431 W which also accounts for around 76.68% of the total exergy destruction rate of the solar ORC. The expander is the second highest source of the exergy destruction rate with a value of 95 W and this value represents 16.9% of the total exergy destruction rate. It is followed by the condenser (32.3 W) and the pump (3.8 W) respectively. These results highlight that more attention should be given to the flat plate collector which is the heat source of the solar ORC in order to enhance the system efficiency. The components of the cycle: flat-plate collector, expander, condenser and pump exergy efficiencies are estimated at 43.57%, 60.7%, 67.3% and 64.73% respectively. The overall energy and exergy efficiency of the solar ORC is calculated as 3.81% and 17.8% respectively. The parametric analysis study also demonstrates that an increase in expander inlet pressure and the degree of superheat have a positive impact on the first and second law efficiency of the solar ORC. Finally, these results show that small scale solar thermal systems, which utilises a flat plate collector can be used to generate not only mechanical work but also heat energy at the same time. Furthermore, environmentally friendly working fluid HFE 7000 offers a feasible alternative to be utilised in small scale solar thermal systems.

Acknowledgement

The authors acknowledge full financial and in-kind support provided by Future Energy Source (FES) Ltd., UK and are thankful to Bournemouth University for their support.

References

- [1] Reddy VS, Kaushik S, Ranjan K, Tyagi S. State-of-the-art of solar thermal power plants—a review. *Renew Sustain Energy Rev* 2013;27:258–73.
- [2] Baharoon DA, Rahman HA, Omar WZW, Fadhl SO. Historical development of concentrating solar power technologies to generate clean electricity efficiently – a review. *Renew Sustain Energy Rev* 2015;41:996–1027.
- [3] Mekhilef S, Saidur R, Safari A. A review on solar energy use in industries. *Renew Sustain Energy Rev* 2011;15:1777–90.
- [4] García-Rodríguez L, Blanco-Gálvez J. Solar-heated Rankine cycles for water and electricity production: POWERSOL project. *Desalination* 2007;212:311–8.
- [5] Zarza E, Valenzuela L, Leon J, Hennecke K, Eck M, Weyers H-D, et al. Direct steam generation in parabolic troughs: final results and conclusions of the DISS project. *Energy* 2004;29:635–44.
- [6] Fernandez-Garcia A, Zarza E, Valenzuela L, Pérez M. Parabolic-trough solar collectors and their applications. *Renew Sustain Energy Rev* 2010;14:1695–721.
- [7] Abbas R, Martínez-Val J. Analytic optical design of linear Fresnel collectors with variable widths and shifts of mirrors. *Renew Energy* 2015;75:81–92.
- [8] Yaqi L, Yaling H, Weiwei W. Optimization of solar-powered Stirling heat engine with finite-time thermodynamics. *Renew Energy* 2011;36:421–7.
- [9] Wang X, Zhao L, Wang J, Zhang W, Zhao X, Wu W. Performance evaluation of a low-temperature solar Rankine cycle system utilizing R245fa. *Sol Energy* 2010;84:353–64.
- [10] Tchanche BF, Lambrinos G, Frangoudakis A, Papadakis G. Low-grade heat conversion into power using organic Rankine cycles – a review of various applications. *Renew Sustain Energy Rev* 2011;15:3963–79.
- [11] Rayegan R, Tao Y. A procedure to select working fluids for Solar Organic Rankine cycles (ORCs). *Renew Energy* 2011;36:659–70.
- [12] Marion M, Voicu I, Tiffonnet A-L. Study and optimization of a solar subcritical organic Rankine cycle. *Renew Energy* 2012;48:100–9.
- [13] Manolakos D, Papadakis G, Mohamed ES, Kyritsis S, Bouzianan K. Design of an autonomous low-temperature solar Rankine cycle system for reverse osmosis desalination. *Desalination* 2005;183:73–80.
- [14] Manolakos D, Papadakis G, Kyritsis S, Bouzianan K. Experimental evaluation of an autonomous low-temperature solar Rankine cycle system for reverse osmosis desalination. *Desalination* 2007;203:366–74.
- [15] Manolakos D, Kosmadakis G, Kyritsis S, Papadakis G. On site experimental evaluation of a low-temperature solar organic Rankine cycle system for RO desalination. *Sol Energy* 2009;83:646–56.
- [16] Bryszewska-Mazurek A, Świeboda T, Mazurek W. Performance analysis of a solar-powered organic rankine cycle engine. *J Air Waste Manage Assoc* 2011;61:3–6.
- [17] Wang J, Zhao L, Wang X. An experimental study on the recuperative low temperature solar Rankine cycle using R245fa. *Appl Energy* 2012;94:34–40.
- [18] Wang J, Zhao L, Wang X. A comparative study of pure and zeotropic mixtures in low-temperature solar Rankine cycle. *Appl Energy* 2010;87:3366–73.
- [19] Zhang X-R, Yamaguchi H, Uneno D. Experimental study on the performance of solar Rankine system using supercritical CO₂. *Renew Energy* 2007;32:2617–28.
- [20] Yamaguchi H, Zhang X, Fujima K, Enomoto M, Sawada N. Solar energy powered Rankine cycle using supercritical CO₂. *Appl Therm Eng* 2006;26:2345–54.
- [21] Dincer I, Rosen MA. Exergy: energy, environment and sustainable development. Newnes; 2012.
- [22] Helvacı HU, Akkurt GG. Thermodynamic performance evaluation of a geothermal drying system. In: Progress in exergy, energy, and the environment. Springer; 2014. p. 331–41.
- [23] Singh N, Kaushik S, Misra R. Exergetic analysis of a solar thermal power system. *Renew Energy* 2000;19:135–43.
- [24] Al-Sulaiman FA. Exergy analysis of parabolic trough solar collectors integrated with combined steam and organic Rankine cycles. *Energy Convers Manage* 2014;77:441–9.
- [25] Baghernejad A, Yaghoubi M. Exergoeconomic analysis and optimization of an Integrated Solar Combined Cycle System (ISCCS) using genetic algorithm. *Energy Convers Manage* 2011;52:2193–203.
- [26] Elsaifi AM. Exergy and exergoeconomic analysis of sustainable direct steam generation solar power plants. *Energy Convers Manage* 2015;103:338–47.
- [27] Helvacı H, Khan ZA. Mathematical modelling and simulation of multiphase flow in a flat plate solar energy collector. *Energy Convers Manage* 2015;106:139–50.
- [28] Bao J, Zhao L. A review of working fluid and expander selections for organic Rankine cycle. *Renew Sustain Energy Rev* 2013;24:325–42.
- [29] Husband W, Beyene A. Low-grade heat-driven Rankine cycle, a feasibility study. *Int J Energy Res* 2008;32:1373–82.
- [30] Tsai W-T. Environmental risk assessment of hydrofluoroethers (HFEs). *J Hazard Mater* 2005;119:69–78.
- [31] Sekiya A, Misaki S. The potential of hydrofluoroethers to replace CFCs, HCFCs and PFCs. *J Fluorine Chem* 2000;101:215–21.
- [32] Qiu G, Shao Y, Li J, Liu H, Riffat SB. Experimental investigation of a biomass-fired ORC-based micro-CHP for domestic applications. *Fuel* 2012;96:374–82.
- [33] Jradi M, Li J, Liu H, Riffat S. Micro-scale ORC-based combined heat and power system using a novel scroll expander. *Int J Low-Carbon Technol* 2014;ctu012.
- [34] Baral S, Kim KC. Thermodynamic modeling of the solar organic Rankine cycle with selected organic working fluids for cogeneration. *Distrib Gener Altern Energy J* 2014;29:7–34.
- [35] Wang Z, Zhou N, Guo J, Wang X. Fluid selection and parametric optimization of organic Rankine cycle using low temperature waste heat. *Energy* 2012;40:107–15.
- [36] Lemmon E, Huber M, McLinden M. NIST reference database 23: reference fluid thermodynamic and transport properties-REFPROP, version 9.1. Standard Reference Data Program; 2013.
- [37] Liu H, Qiu G, Shao Y, Daminabo F, Riffat SB. Preliminary experimental investigations of a biomass-fired micro-scale CHP with organic Rankine cycle. *Int J Low-Carbon Technol* 2010;ctu005.
- [38] Quoilin S. Experimental study and modeling of a low temperature Rankine cycle for small scale cogeneration. University of Liege; 2007.
- [39] Li Y, Wang R, Wu J, Xu Y. Experimental performance analysis on a direct-expansion solar-assisted heat pump water heater. *Appl Therm Eng* 2007;27:2858–68.
- [40] Bejan A. Advanced engineering thermodynamics, 1997. New York: Interscience; 1996.
- [41] Cengel YA, Boles MA, Kanoğlu M. Thermodynamics: an engineering approach. New York: McGraw-Hill; 2002.
- [42] Dikici A, Akbulut A. Performance characteristics and energy–exergy analysis of solar-assisted heat pump system. *Build Environ* 2008;43:1961–72.

- [43] Gupta M, Kaushik S. Exergy analysis and investigation for various feed water heaters of direct steam generation solar–thermal power plant. *Renew Energy* 2010;35:1228–35.
- [44] Freeman J, Hellgardt K, Markides CN. An assessment of solar-powered organic Rankine cycle systems for combined heating and power in UK domestic applications. *Appl Energy* 2015;138:605–20.
- [45] Tchanche B, Lambrinos G, Frangoudakis A, Papadakis G. Exergy analysis of micro-organic Rankine power cycles for a small scale solar driven reverse osmosis desalination system. *Appl Energy* 2010;87:1295–306.
- [46] Tchanche BF, Papadakis G, Lambrinos G, Frangoudakis A. Fluid selection for a low-temperature solar organic Rankine cycle. *Appl Therm Eng* 2009;29:2468–76.